TU/e EINDHOVEN UNIVERSITY OF TECHNOLOGY

Analysis of motional eddy currents in the slitted stator core of an axial-flux permanent magnet machine

Citation for published version (APA):
Friedrich, L. A. J., Gysen, B. L. J., Jansen, J. W., & Lomonova, E. A. (2020). Analysis of motional eddy currents in the slitted stator core of an axial-flux permanent magnet machine. *IEEE Transactions on Magnetics*, *56*(2), 1-4. Article 8959164. https://doi.org/10.1109/TMAG.2019.2953625

DOI:
10.1109/TMAG.2019.2953625

Document status and date:
Published: 01/02/2020

Document Version:
Typeset version in publisher's lay-out, without final page, issue and volume numbers

Please check the document version of this publication:

• A submitted manuscript is the version of the article upon submission and before peer-review. There can be important differences between the submitted version and the official published version of record. People interested in the research are advised to contact the author for the final version of the publication, or visit the DOI to the publisher's website.
• The final author version and the galley proof are versions of the publication after peer review.
• The final published version features the final layout of the paper including the volume, issue and page numbers.

Link to publication

General rights
Copyright and moral rights for the publications made accessible in the public portal are retained by the authors and/or other copyright owners and it is a condition of accessing publications that users recognise and abide by the legal requirements associated with these rights.

• Users may download and print one copy of any publication from the public portal for the purpose of private study or research.
• You may not further distribute the material or use it for any profit-making activity or commercial gain
• You may freely distribute the URL identifying the publication in the public portal.

If the publication is distributed under the terms of Article 25fa of the Dutch Copyright Act, indicated by the "Taverne" license above, please follow below link for the End User Agreement:

www.tue.nl/taverne

Take down policy
If you believe that this document breaches copyright please contact us at:

openaccess@tue.nl

providing details and we will investigate your claim.

Download date: 21. Mar. 2025

Analysis of Motional Eddy Currents in the Slitted Stator Core of an Axial-Flux Permanent Magnet Machine

L. A. J. Friedrich, B. L. J. Gysen, J. W. Jansen, E. A. Lomonova,.
Department of Electrical Engineering, Eindhoven University of Technology, Eindhoven, the Netherlands.
E-mail: L.Friedrich@tue.nl

This paper concerns the modeling and design of a slitted stator core for single-sided axial-flux permanent-magnet machine application. The stator core is specially designed to maximize the magnetic flux density in the airgap and to minimize the eddy current losses occurring at high rotational speeds. To reduce the effort needed for computing the motional eddy current distribution in the presence of nonlinear material characteristics, a novel method is proposed. It combines the harmonic balance method, which is advantageous for simulating in the frequency domain the steady-state periodic response of a nonlinear system under harmonic excitation, together with a source description that introduces a complex magnetization that mimics the displacement of the permanent magnet array. Following this method, time-domain distributions and losses can be reconstructed accurately with a low number of harmonics. A three-dimensional periodic model of the slotless axial-flux machine is built in the framework of isogeometric analysis and a mixed formulation is employed, which relies on high order Nédélec edge-elements. The proposed model is embedded into a gradient-based optimization problem to determine the optimal shape of the slits in the stator core of the motor. This results in a novel cost-effective solution for improving the efficiency of axial-flux permanent-magnet machines.

Index Terms—**Eddy currents, harmonic analysis, permanent magnet machines, stators, magnetic core.**

I. Introduction

AXIAL-FLUX permanent magnet (AFPM) topology exhibits higher power density and efficiency than traditional radial-flux permanent magnet (RFPM) machines [1]. Compact structure, better cooling capabilities, and adjustable airgap make the AFPM technology an attractive candidate compared to RFPM. Single-sided, double-sided, and multi-stack topologies are possible depending on the application. In this paper, a slotless single-sided topology is considered. This choice is motivated by a simpler design and manufacturing solution, and easier stator and rotor removal process. A lower volume of permanent magnet is required and therefore lower cost solution can be proposed. However, single-sided design suffers from unbalanced axial forces, which can lead to more complex bearing systems and thicker dimensions to avoid deflection. The stator core of the AFPM machine is made of soft-magnetic material which exhibits nonlinear *BH* characteristics and leads to hysteresis losses, eddy current losses and additional excess losses under rotating magnetic fields. Two main design methods are commonly used to reduce these losses, either lamination of the core is performed or high-performance material is used, such as grain-oriented electrical steel (GOES) or soft-magnetic composite materials (SMC). However, in axial-flux topologies, the lamination technique is not possible as the stator core would consist of a large set of concentric iron rings with incrementally increasing diameter, which is difficult to manufacture. The use of SMC core is often preferred with AFPM machines, and the development of such materials has been greatly reducing the core losses. However, SMC has a much higher cost than more common types of steel and does exhibit a lower permeability and saturation level. Such a high-performance material solution is not cost-optimal and leads to poor scalability towards large AFPM machines.

A geometrically accurate and time-efficient model is required to assess the machine performances under design changes. AFPM machines are inherently 3D problems, but 2D simplifications are often proposed to reduce the computational effort [2]–[5]. However, quasi-3D models lack accuracy and robustness with respect to dimension changes, especially when nonlinear characteristics are present and when eddy current losses estimation is of interest. Including motional eddy current effects in the simulation can be done using either time-stepping linearization or time-discretization with the Galerkin method, resulting in 4D models. Both methods lead to large systems of equations and require the development of additional techniques to represent accurately the airgap sliding-interface. Moreover, since nonlinear material characteristics are included, several iterations per time-step are needed. If the steady-state solution is of interest, it is necessary to step through several periods, which makes such a method unusable for optimization problems. By assuming harmonic excitation corresponding to a constant rotational speed, and taking advantage of both time and space periodicity of the solution, the complexity can be reduced to a spatial problem in the frequency domain, using the harmonic balance method. Moreover, since the soft-magnetic material characteristic is nonlinear, the solution can be approximated by means of multiharmonic series.

In this paper, an economical solution for AFPM stator design is proposed. It consists of the trimming of elongated holes, or slits, in the azimuthal direction of the core which is made out of cheap soft-magnetic material *Cogent M270-50A-50Hz*. Slitted cores partially replace the laminations in their role of eddy current barriers, while guaranteeing better structural properties and ease of manufacturing. To simulate the three-dimensional motional eddy-current problem with nonlinear magnetic properties, a modeling approach is proposed which combines the isogeometric framework with the decoupled harmonic balance method. The isogeometric analysis enables the exact representation of three-dimensional curved geometries and slits shapes,

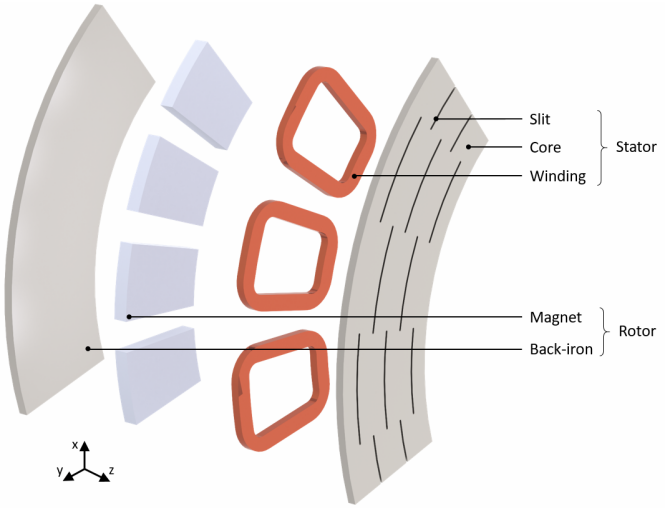

Fig. 1. Periodical section of the single-sided slotless AFPM topology.

as well as the accurate solution of electromagnetic fields on such a complex geometrical structure, at a reduced cost with regards to the number of degrees of freedom, when compared to the traditional finite element method. The multiharmonic system is significantly smaller than its transient counterpart and enables fast and accurate extraction of the machine parameters, such as torque ripples and time-averaged eddy current losses, which are minimized by performing a design optimization of the shape and position of the slits in the stator core of the AFPM machine.

II. Modeling Method

The modeling of the motional eddy currents distribution entails three main components: the geometrical model, the space discretization and finally the matrix assembly for the nonlinear multiharmonic problem. The 3D geometrical model contains curved domains and slits, which are described through B-splines functions. These functions provide a flexible and parametric shape-description, which is also used in CAD models. The different elements are built successively from lines and surfaces to volumes, which are then glued into a multipatch geometry object. The permanent magnet layer exhibits a complex magnetization, where the phase depends on the angular position of the quadrature points. This motionless method mimics the translation of the magnet array and does not need to incorporate a transient solver nor a sliding interface, which eases both the implementation and computational effort.

The quasi-static Maxwell equations are solved for the magnetic vector potential, A, which has all three components active and gauged to ensure a divergence-free solution. This can be done by regularization, i.e. the introduction of an infinitesimal conductivity in non-conducting regions. Instead, a saddle-point approach is chosen in this paper and mixed approximation spaces are constructed for the multipatch geometry. The vectorial basis functions consist of high order *curl*-conforming Nédélec edge-elements, which is a natural choice since only the tangential component of the magnetic vector potential is continuous at the interfaces. The scalar basis function consists of *grad*-conforming elements. Mathematical explanations about the *de Rham* cohomology, the high-order generalization of mixed spaces, and the functional analysis necessary for a complete derivation of the three-dimensional electromagnetic problems modeling in the isogeometric analysis framework can be found in [6].

The mixed formulation relies on the following pair of functional spaces:

$$\mathrm{H}_0(\mathbf{grad},\Omega) = \left\{u \in L^2(\Omega), \nabla u \in L^2(\Omega), u|_{\partial\Omega}= 0\right\}, \quad (1)$$
$$\mathbf{H}_0(\mathbf{curl},\Omega) = \left\{\mathbf{u} \in \mathbf{L}^2(\Omega), \nabla\times\mathbf{u} \in \mathbf{L}^2(\Omega), \mathbf{n}\times\mathbf{u}|_{\partial\Omega}= 0\right\}.$$

The scalar space is used for the Lagrange multipliers, λ, which resemble an electric scalar potential, V, while the vector space is used for the magnetic vector potential A. For each harmonic, k, and each iteration, p, the problems reads:
For $(k,p) \in \mathbb{Z}\times\mathbb{N}$, find $(A_k^{p+1}, \lambda_k^{p+1}) \in \mathbf{H}_0(\mathbf{curl},\Omega) \times \mathrm{H}_0(\mathbf{grad},\Omega)$, such that

$$\begin{bmatrix} S^p_{\nu_0'} + kM & C \\ C^T & 0 \end{bmatrix} \begin{bmatrix} A_k^{p+1} \\ \lambda_k^{p+1} \end{bmatrix} = \begin{bmatrix} I^p_{k,rhs} \\ 0 \end{bmatrix}, \quad (2)$$

with

$$S^p_{\nu_0'\ i,j} = \int_\Omega \nu'^p_0(\mathbf{x})\ \nabla\times\boldsymbol{\omega_j}\cdot\nabla\times\boldsymbol{\omega_i}\ d\mathbf{x}, \quad (3)$$
$$M_{i,j} = \int_\Omega j\omega\sigma\ \boldsymbol{\omega_j}\cdot\boldsymbol{\omega_i}\ d\mathbf{x}, \qquad \boldsymbol{\omega_j} \in \mathbf{H}_0(\mathbf{curl},\Omega), \quad (4)$$
$$C_{i,j} = \int_\Omega \epsilon\ \boldsymbol{\omega_j}\cdot\nabla p_i\ d\mathbf{x}, \qquad p_i \in \mathrm{H}_0(\mathbf{grad},\Omega). \quad (5)$$

where, ν_0', represents the DC component of the incremental magnetic reluctivity, j, is the complex unit vector, ω, is the electrical pulsation, σ, is the electrical conductivity only present in the core denoted Ω_c. The parameter, $\epsilon = 1 + j\omega\sigma$, is a coefficient introduced to gauge the magnetic vector potential in the whole domain Ω and at the same time to gauge the eddy currents in the electrically conducting domain Ω_c.

The harmonic balance method [7], [8], is employed to obtain the coupled system of equation for solving the nonlinear multiharmonic problem. This iterative method has been widely used to model motionless nonlinear systems under harmonic current excitation, such as transformers [9], [10]. However, in this paper, because of the introduction of the source description using complex position-dependent magnetization, the motional eddy currents can be analyzed. The complex-valued problem derived from the harmonic balance is linearized using the fixed-point method described in [11]. The solution in the time-domain is reconstructed from the computed Fourier coefficients. Moreover, the resulting algebraic system is 2N+1 times larger than the original spatial system, where N is the highest harmonic considered in the solution. Therefore, an iterative solver is needed to invert such a matrix, which in turns necessitates proper preconditioner and smoother [10]. In order to limit the implementation overhead, a decoupled harmonics system is chosen, where each harmonic is solved after another, and the inter-harmonic coupling part is done through an equivalent source term, and the right-hand side. The

derivation of the multi-harmonic model falls from the Fourier transform of the diffusion equation (6) which reads

$$\nabla \times (\nu'(A(t))\nabla \times A(t)) - \sigma \frac{\partial A(t)}{\partial t} = \nabla \times \nu' M(t), \quad (6)$$

$$\nabla \times (\mathcal{F}(\nu') * \nabla \times \mathcal{F}(A)) - \sigma \frac{\partial \mathcal{F}(A)}{\partial t} = \nabla \times \mathcal{F}(\nu' M), \quad (7)$$

$$\nabla \times (\sum_{i=-N}^{N} \nu'_{k-i} \nabla \times A_i) - kj\omega\sigma A_k = \nabla \times \nu' M_k, \quad (8)$$

$$\nabla \times (\nu'_0 \nabla \times A_k) - kj\omega\sigma A_k = \nabla \times \nu' M_k \ \ldots - \nabla \times (\sum_{\substack{i=-N \\ i\neq k}}^{N} \nu'_{k-i} \nabla \times A_i), \quad (9)$$

$$[\boldsymbol{S}_{\boldsymbol{\nu}'_0} + k\boldsymbol{M}] A_k^{p+1} = I_{k,rhs}^{p} = \nabla \times \nu' M_k - \sum_{\substack{i=-N \\ i\neq k}}^{N} \boldsymbol{S}_{\boldsymbol{\nu}'_{k-i}} A_i^p. \quad (10)$$

where $\mathcal{F}$ denotes the Fourier transform, $*$ is the convolution product. M indicates the magnetization coefficients in the magnet and the nonlinear iron material, and, ν', indicates the reluctivity coefficients which are obtained through FFT of the reconstructed time profiles at each node.

Correspondingly, the machine performance indicators are reconstructed in the time-domain. The torque profile, T, is obtained through the integration of the Maxwell Stress Tensor with the radius, r, at the interface, $\mathcal{S}$, between the airgap and the core, from the viewpoint of the air:

$$T = \frac{1}{2\mu_0} \oint_{\mathcal{S}} r \, \mathrm{Re}(B_\theta \overline{B_z}) \, \mathrm{d}S. \quad (11)$$

The eddy current losses, P, are obtained through integration of the eddy current density, J, in the core material

$$P = \frac{1}{2\sigma} \int_{\Omega_c} \mathrm{Re}(J\bar{J}) \, \mathrm{d}V. \quad (12)$$

III. Results

The dimensions of the considered AFPM topology and the physical parameters are given in Table I. The model is first validated against a nonlinear transient finite element analysis conducted on the commercial software Altair Flux, which solves the $T-\Phi$ formulation on a second-order hexahedral relaxed mapped-mesh, which includes 273 656 nodes. The validation of the eddy current losses is given in Fig. 2, for the slitless topology. A good match is observed, with a discrepancy on the mean value of the losses equal to 0.97%, 0.42%, 0.51%, and 1.20% for the plate with zero, one, two and three slits, respectively. However, different phase-shifts can be observed and explained by the fact that the harmonic balance solves the Fourier coefficients without information about the initial phase useful for the reconstruction. To remedy this issue, several methods exist that extend the algebraic system by one or more additional equations to gauge the phase value [12], [13]. Concerning the computational time, different implementation platforms and strategies are considered so the validity of the comparison should be taken relatively carefully. In FEM, the transient problem is simulated on 3 periods, with 20 time-steps per period to ensure the steady-state is reached. The computational effort for solving the nonlinear system is about 3 days. This effort only includes the solving time, in particular, no meshing and post-processing are considered. In IGA, the computational effort is about 80s, 160s, 250s, and 340s, for the topologies with zero, one, two and three slits, respectively. This computational time includes the creation of the geometry, the generation of the functional spaces and mesh, the solving, and the post-processing. The computational effort of the transient FEM is considered as impractical for design optimization compared to the proposed frequency-domain approach.

TABLE I
Initial parameters of the considered AFPM topology

Parameter	Value	Parameter	Value
Back-iron height	6 mm	Pole-pair number	9
Magnet height	11 mm	ω_m	1500 rpm
Airgap and coil height	6 mm	σ	$1.\overline{81}$ S/mm
Core height	45 mm	B_{rem}	1.35 T
Magnet filling	0.8	μ_{pm}	1.05
Inner air radius	60 mm	μ_{iron}	300
Inner core radius	90 mm	Slit arc-to-pitch ratio	1/3
Inner magnet radius	95 mm	Slit thickness	2 mm
Outter magnet radius	156 mm	First slit radius	110 mm
Outter core radius	161 mm	Second slit radius	125 mm
Outter air radius	191 mm	Third slit radius	140 mm

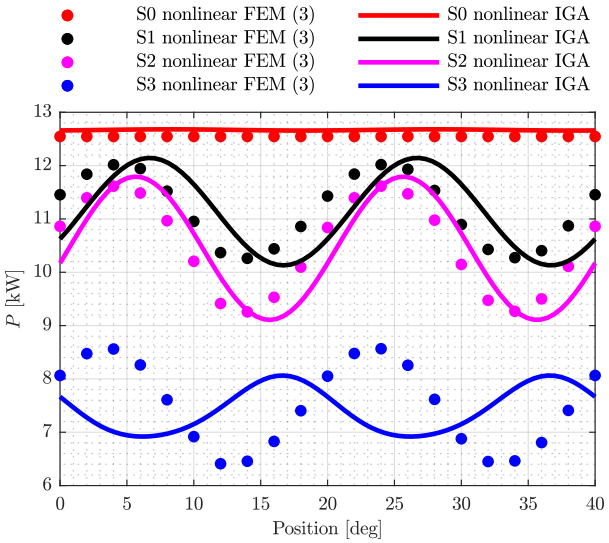

Fig. 2. Eddy current losses validation for the initial topology with no slit (S0), one slit (S1), two slits (S2), and three slits (S3).

The validated model is further embedded in a gradient-based optimization problem. The design variables, $\vec{x_i}$, controls the control points of the B-splines which determine the shape and position of the slits. The objective consists in the minimization of the mean eddy current losses, P_{eddy}, while maintaining a low magnitude of torque ripples, T_{rip}. The optimization problem reads:

$$\text{For } i \in [1,3], \underset{\vec{x_i}=\{R_j,\alpha_j\} \ j\in[1,i]}{\text{minimize:}} \quad P_{eddy}(\vec{x_i}), \ T_{rip}(\vec{x_i}) < 10\% \quad (13)$$

where R_j and α_j are the radii and the arc-to-pitch ratios of each slit. The result of the optimization together with the original

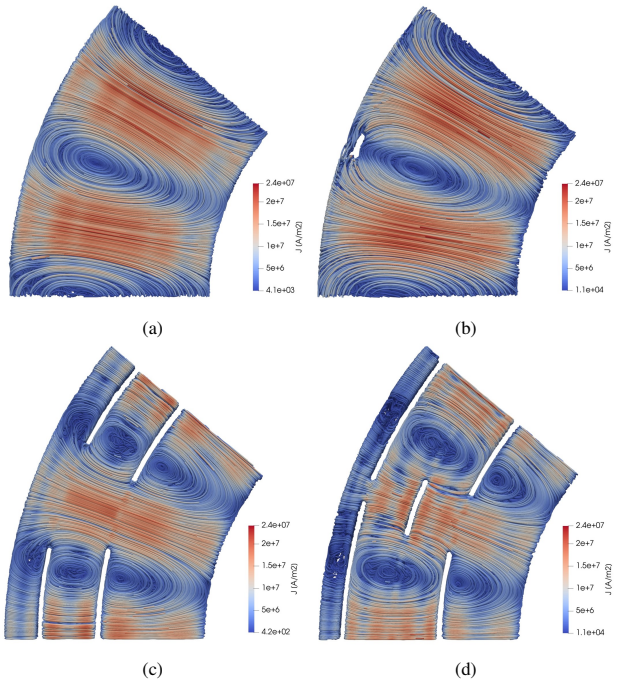

Fig. 3. Eddy current density distribution in [A/m^2] obtained with the proposed method for the optimized topologies with (a) no slit, (b) one slit, (c) two slits and (d) three slits.

values of the eddy current losses and the torque ripples are summarized in Table II. Moreover, on Fig. 3(a), the eddy current density distributions are shown in the slitless plate, and the influence of the number of slits is exemplified on Figs. 3(b)-(d). It can be observed, that the eddy current losses can be reduced by 51%, 87% and 97%, by introducing one, two, or three slits, respectively. This demonstrates the applicability and flexibility of the proposed approach, as a computationally efficient framework for solving nonlinear motional eddy current problems. The slit thickness was fixed to 2mm to ease visualization, however, in practical applications, it should be minimized since it impairs the magnetic loading and the developed torque. Additionally, the number of slits should be further increased to reduce the eddy current losses towards a more practical value for the considered application. To treat the slitted-stator problem more efficiently, it is beneficial to be able to describe an increasing number of slits without changing dramatically the number of patches and the computational time. This can be achieved through boolean trimming operations and the use of hybrid high-order mesh elements, which are active research topics in the context of IGA [14], [15]. Finally, hierarchical vector spaces are of interest, as they allow to refine adaptively the mesh in the skin-depth of the core, where the eddy currents are concentrated [16].

IV. Conclusion

A source description relying on the use of a complex-valued magnetization has been proposed, which allows computing the eddy current distribution in the stator core due to the motion of a permanent magnet array, in the frequency domain. This extends the application of the harmonic balance method to model motional eddy currents in the presence of nonlinear material characteristics. This method is applied to the modeling and design of slits in the core, which act as eddy current barriers and increase the efficiency of the AFPM machine. Slitted stator core offers a novel cost-effective solution for the manufacturing of permanent magnet machines.

TABLE II
Performance indicators comparison

Number of slits	Initial		Optimized	
	P_{eddy} [kW]	T_{rip} [%]	P_{eddy} [kW]	T_{rip} [%]
0	12.55	0.28	-	-
1	11.31	18.09	6.04	4.19
2	10.44	25.70	1.56	5.00
3	7.43	15.40	0.39	6.12

References

[1] C. W. Kim, G. H. Jang, J. M. Kim, J. H. Ahn, C. H. Baek, and J. Y. Choi, "Comparison of axial flux permanent magnet synchronous machines with electrical steel core and soft magnetic composite core," *IEEE Transactions on Magnetics*, vol. 53, no. 11, pp. 1-4, Nov. 2017.

[2] J. S. Kim, J. H. Lee, J. Y. Song, D. W. Kim, Y. J. Kim, and S. Y. Jung, "Characteristics analysis method of axial flux permanent magnet motor based on 2-d finite element analysis," *IEEE Transactions on Magnetics*, vol. 53, no. 6, pp. 1-4, June 2017.

[3] A. A. Arkadan, T. M. Hijazi, and B. Masri, "Design evaluation of conventional and toothless stator wind power axial-flux pm generator," *IEEE Transactions on Magnetics*, vol. 53, no. 6, pp. 1-4, June 2017.

[4] J. W. Jung, H. I. Park, J. P. Hong, and B. H. Lee, "A novel approach for 2-d electromagnetic field analysis of surface mounted permanent magnet synchronous motor taking into account axial end leakage flux," *IEEE Transactions on Magnetics*, vol. 53, no. 11, pp. 1-4, Nov. 2017.

[5] W. Tong, S. Wang, S. Dai, S. Wu, and R. Tang, "A quasi-three-dimensional magnetic equivalent circuit model of a double-sided axial flux permanent magnet machine considering local saturation," *IEEE Transactions on Energy Conversion*, vol. 33, no. 4, pp. 2163-2173, Dec. 2018.

[6] L. Beirão da Veiga, A. Buffa, G. Sangalli, and R. Vázquez, "Mathematical analysis of variational isogeometric methods," *Acta Numerica*, vol. 3, pp. 157-287, 2014.

[7] S. Yamada, P. Biringer, and K. Bessho, "Calculation of nonlinear eddy-current problems by the harmonic balance finite element method," *IEEE Transactions on Magnetics*, vol. 27, no. 5, pp. 4122–4125, 1991.

[8] J. Driesen, G. Deliège, T. van Craenenbroeck, and K. Hameyer "Implementation of the harmonic balance finite element method for large-scale saturated electromagnetic devices," *Transactions on Engineering Sciences*, vol. 22, pp. 1-10, 1999.

[9] O. Biro, G. Koczka and K. Preis, "Fast time-domain finite element analysis of 3-D nonlinear time-periodic eddy current problems with T, $\Phi - \Phi$ formulation," *IEEE Transactions on Magnetics*, vol. 47, no. 5, pp. 1170-1173, May 2001.

[10] F. Bachinger, U. Langer and J. Schöberl, "Efficient solvers for nonlinear time-periodic eddy current problems," *Computing and Visualization in Science*, vol. 9, no. 4, pp. 197–207, 2006.

[11] L. A. J. Friedrich, M. Curti, B. L. J. Gysen and E. A. Lomonova, "High-order methods applied to nonlinear magnetostatic problems," *Mathematical and Computational Applications*, vol. 24, no. 19, pp. 1–15, Jan. 2019.

[12] R. J. Pogorzelski and A. Georgiadis, Coupled-oscillator based active-array antennas, *John Wiley & Sons*, vol. 11, 2012.

[13] A. Suárez, Analysis and design of autonomous microwave circuits, *John Wiley & Sons*, vol. 190, 2009.

[14] F. de Prenter, C. V. Verhoosel, G. J. van Zwieten, and E. H. van Brummelen, "Condition number analysis and preconditioning of the finite cell method," *Computer Methods in Applied Mechanics and Engineering*, 316:297-327, April 2017.

[15] P. Antolin, A. Buffa, and M. Martinelli, "Isogeometric Analysis on V-reps: first results," *arXiv preprint:1903.03362*, March 2019.

[16] L. A. J. Friedrich, B. L. J. Gysen, M. G. L. Roes and E. A. Lomonova, "Adaptive Isogeometric Analysis applied to an electromagnetic actuator," *IEEE Transactions on Magnetics*, vol. 55, no. 06, June 2019.